

Dalton Transactions

Accepted Manuscript

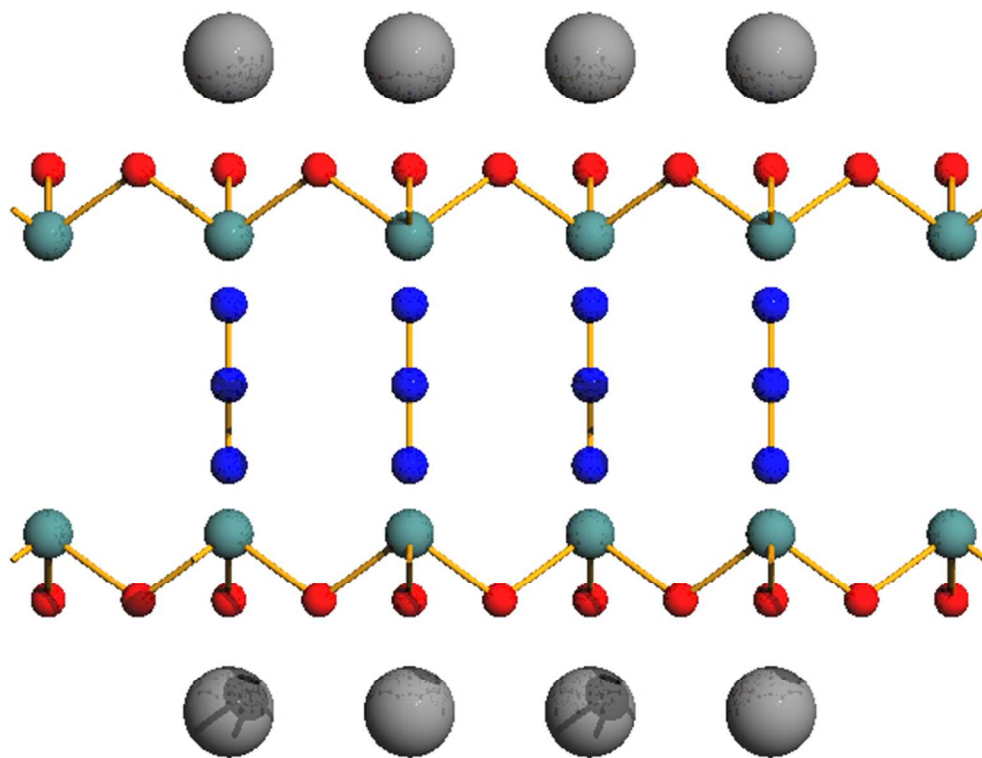


This is an *Accepted Manuscript*, which has been through the Royal Society of Chemistry peer review process and has been accepted for publication.

Accepted Manuscripts are published online shortly after acceptance, before technical editing, formatting and proof reading. Using this free service, authors can make their results available to the community, in citable form, before we publish the edited article. We will replace this *Accepted Manuscript* with the edited and formatted *Advance Article* as soon as it is available.

You can find more information about *Accepted Manuscripts* in the [Information for Authors](#).

Please note that technical editing may introduce minor changes to the text and/or graphics, which may alter content. The journal's standard [Terms & Conditions](#) and the [Ethical guidelines](#) still apply. In no event shall the Royal Society of Chemistry be held responsible for any errors or omissions in this *Accepted Manuscript* or any consequences arising from the use of any information it contains.



Two novel arsenic(III) oxide intercalates with potassium and ammonium azides have been synthesized and their crystal structures have been determined.

Cite this: DOI: 10.1039/c0xx00000x

www.rsc.org/xxxxxx

ARTICLE TYPE

Structure and energetics of arsenic(III) oxide intercalated by ionic azides

Piotr A. Guńka,*^a Karol Kraszewski,^a Yu-Sheng Chen^b and Janusz Zachara^a

Received (in XXX, XXX) Xth XXXXXXXXXX 20XX, Accepted Xth XXXXXXXXXX 20XX

DOI: 10.1039/b000000x

Unprecedented intercalates of arsenic(III) oxide with potassium azide and ammonium azide have been obtained and characterized by single crystal X-ray diffraction. The compounds are built of As₂O₃ sheets separated by charged layers of cations and azide anions perpendicular to the sheets. The intercalates are an interesting example of hybrid materials whose structure is governed by covalent bonds in two directions and ionic bond in the third one. Obtained compounds are the first example of As₂O₃ intercalates containing linear pseudohalogen anions. Periodic DFT calculations of interlayer interaction energies were carried out with the B3LYP-D* functional. The layers are held together mainly by ionic bond, although the computations indicate that interactions between cations and As₂O₃ sheets also play a significant role. Comparison of cation and anion interaction energies with neutral As₂O₃ sheets sheds light on crystallisation process, indicating the templating effect of potassium and ammonium cations. It consists in the formation of sandwich complexes of cations with crown-ether-resembling As₆O₁₂ rings. Raman spectra of both compounds are recorded and computed *ab initio* and all vibrational bands are assigned.

Introduction

Intercalation compounds result from inclusion, without covalent bonding, of molecules or ions in a solid matrix of another compound which has a layered structure.¹ Intercalates of various inorganic hosts exhibit a wide range of interesting properties and find numerous every-day applications. Lithium intercalates of transition-metal-based materials such as LiMnO₂, LiCoO₂ and FePO₄ are utilised as electrodes in lithium-ion batteries,^{2,3} whereas iron arsenide and iron selenide based intercalates with metals or with metals and organic solvents can be superconducting at temperatures as high as ~50 K.⁴⁻⁸ The alkali metals intercalates of graphite are used as reducing agents in chemical synthesis.⁹ There is a number of arsenic(III) oxide intercalates described in the literature whose crystal structures have been determined. These include hexagonal KX·2As₂O₃ where X=Cl, Br, I; NH₄Y·2As₂O₃ where Y=Br, I;¹⁰ hydrated 2NH₄Cl·4As₂O₃·H₂O¹¹ and orthorhombic NaBr·2As₂O₃.¹² To the best of our knowledge, there are no publications reporting intercalates with other types of ions, particularly non-spherical ones. We have, therefore, attempted to synthesise arsenic(III) oxide intercalates with salts containing ions with different geometry and, herein, we report the synthesis and crystal structures of the first As₂O₃ intercalates containing linear pseudohalogen anions. In order to understand the contribution of various components to the interlayer interaction energies, we have performed periodic DFT computations with the B3LYP-D* functional. Moreover, we show experimental Raman spectra of the intercalates with all the bands assigned by comparison with theoretical vibrational frequencies.

Experimental and computational details

All chemicals used, except for NH₄AsO₂ which was synthesized as described previously,¹³ were obtained from commercial sources and were used as received, without further purification. Reactions were carried out in open glass vessels.

NH₄N₃·2As₂O₃ (1). NH₄AsO₂ crystals were stored at 5°C after the synthesis in a closed vessel in a saturated aqueous solution of ammonium arsenite. 75 mg of the crystals were taken together with 0.5 mL of the solution and were mixed with a solution of 98 mg of NaN₃ in 3 mL of water. The mixture was stirred until all ammonium arsenite was dissolved and the resulting solution was left for crystallisation via slow water evaporation. When a third of the initial solution volume was left in the vessel, crystallisation was stopped yielding single crystals of compound **1** exclusively with a yield of 60%.

KN₃·2As₂O₃ (2). 0.4 g of As₂O₃ powder (2 mmol) was added to 3 ml of 2M KOH solution (6 mmol) and stirred until all As₂O₃ was dissolved. Afterwards, 0.13 g of NaN₃ (2 mmol) was dissolved in the solution. Then, concentrated HNO₃ solution was added dropwise until a solid phase precipitated (pH ~ 9-10 was achieved at this point). The resulting powder was filtered and washed with a mixture of methanol and concentrated HNO₃ (9:1, *V/V*) twice. The powder was dried on filter paper. Such a procedure leads to pure intercalate **2** with a yield of 65%. In order to grow single crystal suitable for X-ray diffraction experiment, the solution was diluted five times before the addition of HNO₃. Nonetheless, all attempts led to tiny, plate-shaped single crystals whose diffraction pattern was only measurable using synchrotron X-ray

Cite this: DOI: 10.1039/c0xx00000x

www.rsc.org/xxxxxx

ARTICLE TYPE

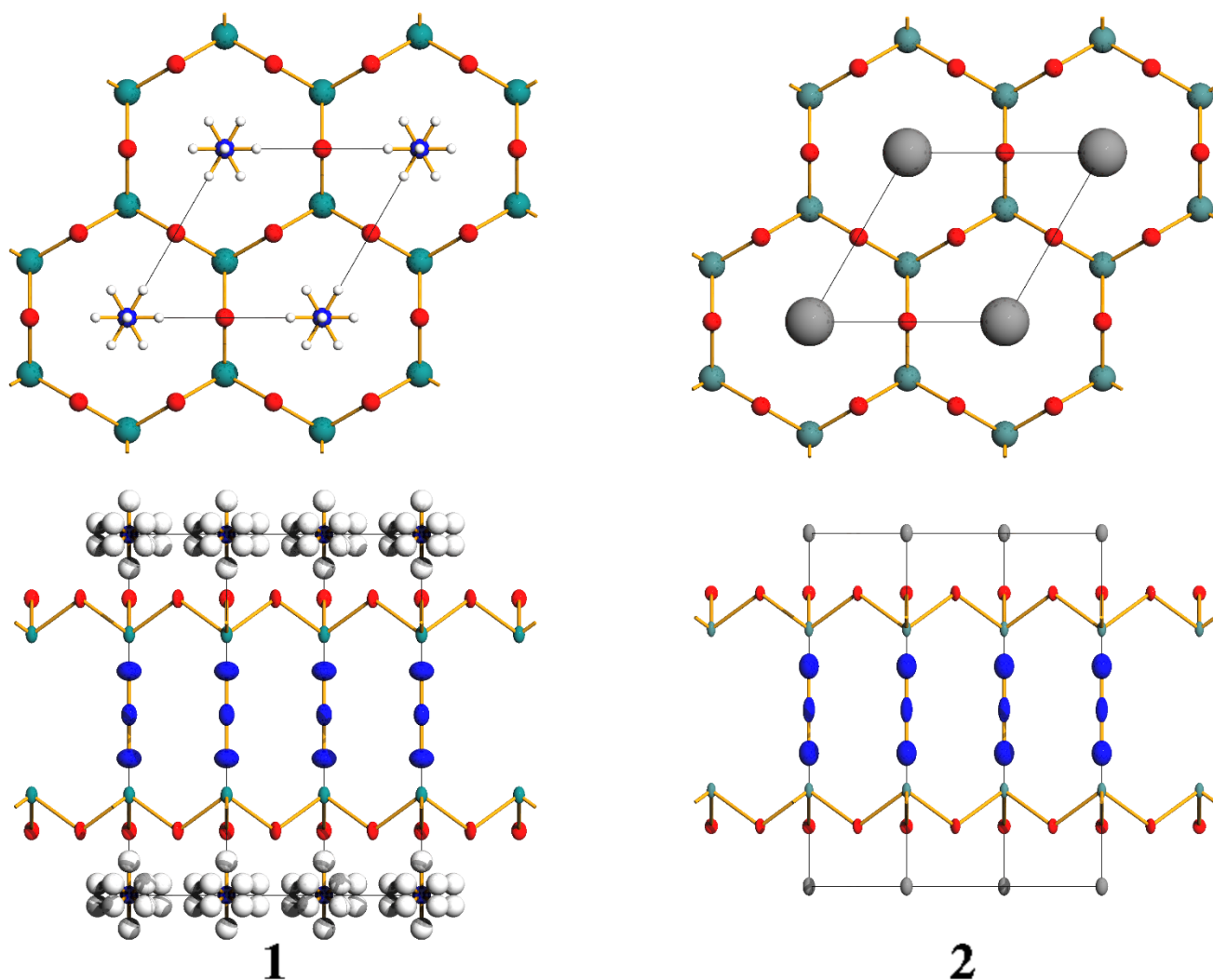


Fig. 1 Crystal structures of intercalates **1** and **2**. View along the [001] direction in a ball and stick model and view along the [120] direction with ADPs visualised are presented at the top and at the bottom, respectively. Thermal ellipsoids are drawn at the 50% probability level.

source.

Suitable single crystals were selected under a polarizing microscope, mounted in inert oil and transferred to the cold gas stream of the diffractometer. Diffraction data for compound **1** were measured at RT with graphite-monochromated Mo-K α radiation on the Oxford Diffraction κ -CCD Gemini A Ultra diffractometer. Absorption effects were corrected analytically.¹⁴ Cell refinement and data collection as well as data reduction and analysis were performed with the Oxford Diffraction software CrysAlis^{PRO}.¹⁵ Diffraction data for compound **2** were collected at ChemMatCARS beamline, 15-ID-B, at the Advanced Photon Source (APS), U.S.A. A Bruker APEXII CCD detector was used to record the diffracted intensities at $\lambda = 0.38745$ Å (32 keV) and at the following temperatures 45(2), 35(2), 25(2), 15(2) and 30(2)

K. Data reduction and analysis including multi-scan absorption and oblique corrections were carried out using the APEX-II suite and SADABS.¹⁶ The structures were solved by direct methods and subsequent Fourier-difference synthesis and refined by full-matrix least-squares against F^2 with SHELX-2013¹⁷ within the Olex2 suite which was also used for data analysis.¹⁸ Ammonium cations in compound **1** lie on a special position exhibiting $6/mmm$ site symmetry and, hydrogen atoms, are disordered. Figures of crystal structures were created using Diamond¹⁹ and rendered with POV-Ray.²⁰ All of the discussions on crystal structure of compound **2** relate to the 45 K measurement, if not stated otherwise.[‡] Raman spectra were recorded using Nicolet Almega Dispersive Raman spectrometer. Spectra of powders of **1** and **2** were

obtained using 780 nm excitation line and a 1200 lines/mm resolution grating. The exposition time was 30 s.

Periodic quantum mechanical computations were carried out using the CRYSTAL09 programme suite.^{21–23} Calculations were performed within the DFT^{24,25} framework using the hybrid B3LYP functional²⁶ with an all-electron TZVP basis set optimised for solid state computations (pob-TZVP).²⁷ Dispersion interactions were accounted for by an empirical correction scheme proposed by Grimme²⁸ with a modified parameterisation developed by Civalleri et al. (B3LYP-D* model).²⁹ The five tolerances setting the accuracy of the Coulomb and exchange series were arbitrarily set to 7, 7, 7, 7, 25 and SCF convergence on the total energy was set to 10^{-7} and 10^{-10} hartree for geometry optimisation and for frequency calculations, respectively. The shrinking factor in the reciprocal net was set to 8, an extra-large grid was used for charge integration (XLGRID keyword) and a modified Broyden scheme,³⁰ following the method proposed by Johnson,³¹ was used to speed up SCF convergence. Vibrations were visualized and analysed using J-ICE.³²

Results and discussion

Crystal structures

The first report on the crystal structure of an arsenic(III) oxide intercalate was published in 1950s. It was a hexagonal hydrated intercalate of ammonium chloride.¹¹ Afterwards, in 1980s Pertlik obtained a series of intercalates with ammonium and potassium halides as well as sodium bromide by means of hydrothermal crystallisations. All of the compounds exhibited hexagonal symmetry except for the intercalate with NaBr which crystallised in the orthorhombic crystal system.^{10,12} We have obtained new intercalates from arsenic(III) oxide dissolved in ammonia or potassium hydroxide aqueous solutions containing sodium azide. Crystallisations were effected by RT evaporation of water in case of ammonia solution or by addition of a mineral acid to the KOH solution. In both cases only one crystalline phase was obtained which was confirmed by the comparison of samples' experimental powder diffractograms with ones generated from the determined crystal structures (see Fig. S1 in the Supporting Material). Similarly as the so-far-known intercalates with potassium and ammonium halides, intercalates with NH_4N_3 (**1**) and KN_3 (**2**) crystallise in the $P6/mmm$ space group and their crystal structures are isotypic (see Fig. 1). The As–O bond lengths equal 1.7902(13) Å in compound **1** and 1.793(2) Å in **2** which agrees well with the values reported by Pertlik. For example, As–O distances in NH_4Br and KCl intercalates of As_2O_3 amount to 1.801(1) and 1.793(2) Å, respectively.¹⁰ The As_2O_3 ψ -tetrahedra share all oxygen ligands, forming neutral As_2O_3 sheets, oriented parallel to the (001) lattice planes. The topology of the As_2O_3 layers is the same as in other hexagonal intercalates with potassium and ammonium halides. They are planar and all of the arsenic atomic cores are situated on one side of the plane formed by oxygen ligands. The oxygen side of the sheets is adjacent to a layer of cations and the other side, where pendent arsenic lone electron pairs (LEPs) are situated, interacts with azide anions perpendicular to the sheets. This results in a periodic pattern of neutral As_2O_3 sheets and alternating ionic layers (see Fig. 1). The As \cdots N separations are 3.178(2) Å for **1**

and 3.189(5) for **2** which is a little less than sum of arsenic and nitrogen van der Waals radii (3.40 Å), indicating the presence of weak interactions between arsenic atoms and azide anions. Similarly as in intercalates with potassium and ammonium halides, the threefold coordination of arsenic atoms by oxygen ligands is complemented by three N_3^- anions, forming a distorted octahedron. A survey of CSD reveals that As \cdots N_3^- contacts shorter than the sum of vdW radii are rather rare. Only one compound with separation of 2.973(3) Å was found (refcode HUGLIE). Nonetheless, there are reports on compounds containing As(III), Sb(III) and Bi(III) coordination centres and azide ligands.^{33–36} The azide anions are symmetrical with N–N bond lengths of 1.173(7) and 1.161(16) Å for compounds **1** and **2**, respectively. Such bond lengths are typical for ionic inorganic azides.³⁷

Due to the separation of ions having opposite charge by neutral As_2O_3 sheets, the interionic K \cdots N_{middle} and N \cdots N_{middle} distances of 4.7433(9) and 4.8393(3) Å are much longer than in the KN_3 and NH_4N_3 ionic crystals (3.5372(3) and 3.740(2), respectively).^{37,38} There are quite large voids in the crystal structures, located in ionic layers. The packing indices for compound **1** and **2** equal 80.9% and 88.1%, respectively.

When carrying out diffraction experiments at the APS synchrotron, we noted that the crystals of intercalate **2** broke upon flash-cooling to 15 K which was manifested by the presence of split reflections in their diffraction patterns. Nevertheless, the intercalate crystals remained intact when cryo-cooled to 45 K. Suspecting a polymorphic transition, we decided to undertake a multi-temperature study of the intercalate's crystal structure. We recorded the diffraction patterns of one crystal at the following temperatures in the given order: 45, 35, 25, 15 and 30 K. Reflections recorded at 45 K were not split and cooling the crystal by 10 degrees did not cause any division of reflections. We did not observe any polymorphic transition either. However, unit cell was expanding as a function of irradiation time (equivalent to X-ray dose) and the increase of displacement parameters for terminal nitrogen atoms of azide anions was much more pronounced than for all the other atoms (Fig. S2 and Table S1 in the Supporting Information). Expansion of unit cell and increase of B_{iso} value with accumulating X-ray dose are commonly observed symptoms of radiation damage in protein crystallography.³⁹ This suggests that the studied crystal was subject to radiation damage and it proceeded mainly via decomposition of azide anions probably accompanied by nitrogen evolution.

Interlayer interaction energies

DFT computations with periodic boundary conditions were carried out in the CRYSTAL09 programme suite in order to understand the energetic factors responsible for the formation of a layered structure of intercalates. Both energies of crystal lattices and energies of electrically neutral layers extracted from 3D periodic structures were computed. B3LYP functional was chosen as it is known to describe oxidic and semiconducting solids accurately⁴⁰ and to predict vibrational spectra of inorganic systems well.⁴¹ We have also used the Grimme correction for the dispersion forces (DFT-D2)²⁸ as we expected it to be significant in the case of studied materials.²⁹ The space group symmetry of compound **1** was arbitrarily lowered to $P31m$ for computations to

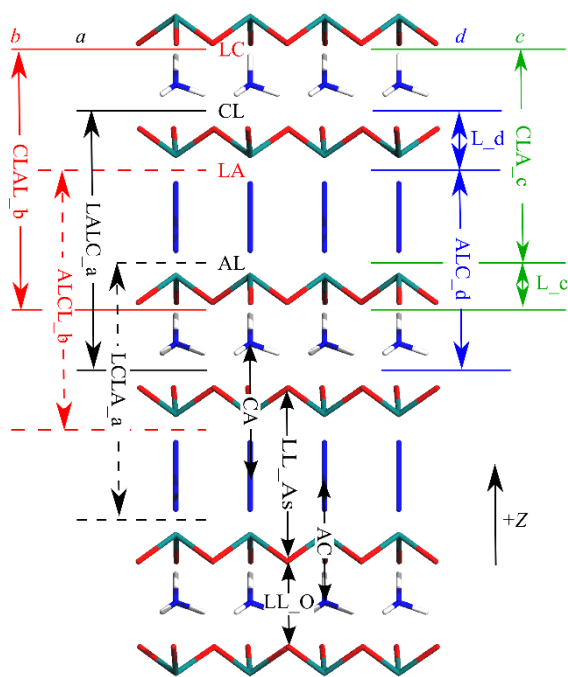


Fig. 2 Possible layer extraction choices and interlayer interaction energies in crystal structures of intercalate **1** and **2**.

circumvent the disorder of ammonium hydrogen atoms. The geometry of layers extracted for interaction energies calculations was kept fixed at the optimised geometry of periodic structures. Two strata of ghost atoms were added on each side of extracted layers when BSSE was estimated according to the BB-CP method.⁴²

There are several possibilities of how to extract electrically neutral layers from the studied intercalates (Fig. 2). The choices may be divided into three groups – layers terminated with an ion on one side only, denoted *a* and *b*, layers terminated with ions on both sides, denoted *c* and *d*, and purely arsenic(III) oxide layers. The *a* and *b* choices of layers as well as the *c* and *d* choices are related by inversion centre. They are unique in the axial *P31m* space group utilised for compound **1** computations and equivalent by symmetry in the centrosymmetric *P6/mmm* space group of compound **2** which reduces the number of possible extractions by two. There are four pairs of interlayer interactions present in the investigated structures – the interactions between cations (C) and As_2O_3 neutral layers (L) with the interaction energies denoted as E_{CL} and E_{LC} (the order of letters is consistent with the $-Z$ direction); the interactions of anions (A) with As_2O_3 layers: E_{AL} and E_{LA} ; ionic interactions E_{CA} and E_{AC} ; and the interactions between neutral As_2O_3 sheets, which we will refer to as $E_{LL_{As}}$ when layers are chosen such that arsenic atoms from adjacent sheets point towards one another and E_{LL_O} otherwise. To compute the interaction energies, we note that unit cell energy can be decomposed into the following terms when layers are extracted according to choices *c* and *d*:

$$\mathcal{E}_0 = \mathcal{E}_{CLA_c} + \mathcal{E}_{L_c} + E_{AC} + E_{LL_O} + E_{LL_{As}} + E_{AL} + E_{LC} \quad (1a)$$

$$\mathcal{E}_0 = \mathcal{E}_{ALC_d} + \mathcal{E}_{L_d} + E_{CA} + E_{LL_O} + E_{LL_{As}} + E_{LA} + E_{CL} \quad (1b)$$

where \mathcal{E}_0 denotes unit cell energy, \mathcal{E}_{L_i} denotes energy of

extracted layer of sequence *I* corresponding to choice *i* and E_{INT} is the interaction energy INT (see Fig. 2 for the clarification of the notation). We find analogous decomposition equations for the choices *a* and *b*:

$$\mathcal{E}_0 = \mathcal{E}_{LALC_a} + E_{CL} + E_{CA} + E_{LL_O} \quad (2a)$$

$$\mathcal{E}_0 = \mathcal{E}_{LCLA_a} + E_{AL} + E_{AC} + E_{LL_{As}} \quad (2b)$$

$$\mathcal{E}_0 = \mathcal{E}_{CLAL_b} + E_{LC} + E_{AC} + E_{LL_O} \quad (2c)$$

$$\mathcal{E}_0 = \mathcal{E}_{ALCL_b} + E_{LA} + E_{CA} + E_{LL_{As}} \quad (2d)$$

In order to estimate the E_{LL_O} and $E_{LL_{As}}$ we extract only the As_2O_3 sheets from intercalate structures and we notice that:

$$\mathcal{E}_{LL_O} = \mathcal{E}_{L_c} + \mathcal{E}_{L_d} + E_{LL_O} \quad (3a)$$

$$\mathcal{E}_{LL_{As}} = \mathcal{E}_{L_c} + \mathcal{E}_{L_d} + E_{LL_{As}} \quad (3b)$$

Note that the following pairs of equations are equivalent by symmetry for compound **2**: (1a) and (1b), (2a) and (2c) as well as (2b) and (2d). The solution of the system of linear equations is straightforward and is given in Table S2 in the Supporting Information. Obtained interaction energy values are presented in Table 1. The optimised structures of compounds **1** and **2** as well as \mathcal{E}_{L_i} values are given in Tables S3 and S4. The BSSE error was estimated using BB-CP method which in practice consists in adding ghost atoms to the extracted layers where additional basis functions are centered.⁴² As can be seen from Table 1, the BSSE error is huge for anion-layer interactions and substantial for cation-layer contacts. This observation agrees well with the conclusion of Brandenburg and co-workers presented in a recent publication where a geometric method of BSSE correction has been extended to periodic DFT calculations.⁴³ It was shown there that BSSE can be enormous for the *pop-TZVP* basis set.

Table 1 Computed interlayer interaction energies for compounds **1** and **2**. E stands for interaction energy, E^C is the BSSE-corrected value and E_{ion} is the electrostatic energy of ionic bond estimated from the Madelung approximation with the EUGEN code. All values are given in kJ/mol per unit cell.

Compound	Interlayer interaction	E	E^C	E_{ion}
1 $\text{NH}_4\text{N}_3 \cdot 2\text{As}_2\text{O}_3$ <i>P31m</i>	CA	-237.5	-233.4	-281.1 ^a
	AC	-237.4	-234.6	-272.3 ^b
	LL_O	-24.9	-24.8	
	LL_As	-14.0	-15.5	
	CL	-55.0	-41.7	
	LC	-37.3	-26.1	
2 $\text{KN}_3 \cdot 2\text{As}_2\text{O}_3$ <i>P6/mmm</i>	CA	-240.1	-234.9	-289.3 ^a
	LL_O	-24.9	-25.1	-273.0 ^b
	LL_As	-14.1	-18.3	
	CL	-68.6	-51.7	
	AL	-32.4	-12.1	
		LA	-30.3	-11.4

^a Both ions were treated as monopoles. ^b Cations were treated as monopoles and azide anions as two -0.5 partial point charges located on terminal nitrogen atoms.

As expected the E_{CA} and E_{AC} electrostatic energies for both compounds are much larger than all the other interlayer interaction energies indicating that it is the ionic bond that is

mainly responsible for holding the layers together in **1** and **2** intercalate crystals. The energy is dependent only on interacting ion charges and their spatial distribution, being independent on the ions' nature. These energies are essentially the same because they can be treated as the Madelung energies of the crystals.^{44–47} The Madelung constants for **1** and **2** are equal as both compounds crystallise in the same invariant crystal structure type. The Madelung energy, on the other hand, depends also on the interionic distances and, hence, the observed differences.⁴⁸ We have computed the electrostatic energy of the ionic NH_4N_3 and KN_3 lattices obtained from the optimised intercalate **1** and **2** structures by removing As_2O_3 sheets. We have used a method for calculating Madelung constants implemented in the EUGEN code.⁴⁹ The electrostatic energy values are given in Table 1. The absolute values obtained from periodic DFT calculations are smaller than the energy evaluated with the EUGEN code, as the DFT values take into account screening by the As_2O_3 sheets. These values are also significantly lower than the lattice energies of ionic NH_4N_3 and KN_3 crystals which amount to -670.3 and -673.2 kJ/mol, respectively (all ions were treated as point charges and crystal structures were taken from ref. 37 and 38). The crystallisation of intercalates causes spatial separation of cations and anions by neutral As_2O_3 sheets leading to a substantial decrease of ionic bond strength. Nonetheless, the studied compounds are an interesting example of hybrid materials whose structures are governed by covalent As–O bonds in two dimensions (*ab* planes) and by ionic bond in the third direction (*Z* axis).

The E_{CL} and E_{LC} energies for compound **1** differ significantly from each other which stems from the fact that different interlayer hydrogen bond motifs are cut in the two cases. In case of the CL boundary, there are three hydrogen atoms pendant from cationic layers, whereas there is only one in case of the LC boundary. The hydrogen atom is in addition less favourably located for hydrogen bond formation than the other three. This results in an interaction energy smaller by 15.6 kJ/mol for boundary LC. Analogous $|E_{AL} - E_{LA}|$ energy difference amounts to as little as 0.7 kJ/mol. Surprisingly, the C··L interaction energies are higher for potassium than for ammonium cations, while A··L interaction energies are very similar in **1** and **2**. It is important to realise that the C··L interlayer interaction energies are much higher than the A··L interaction energies which points to stronger cations interactions with As_2O_3 sheets.

Closer inspection of the 12-fold coordination sphere of potassium and ammonium cations with K··O and N··O distances of 3.0790(19) and 3.1349(14) Å, respectively, reveals its resemblance to cations' coordination by 18-crown-6 ethers, where the K··O and N··O average separations are 2.85(8) and 2.97(7) Å, respectively.⁵⁰ Cation··oxygen distances are lower for the complexes with crown ethers as cations enter the cavity of the chelating ligands while they are sandwiched between two crown-ether-like As_6O_{12} rings in the intercalates. This and the fact that interaction energies with cations are higher than with anions may indicate a templating effect of cations during intercalates crystallisation. It might be assumed that sandwich complexes of cations with six-membered As_6O_{12} rings are formed at the first stage which in turn condense to yield As_2O_3 layers. All of the so-far-studied arsenic(III) oxide intercalates containing potassium

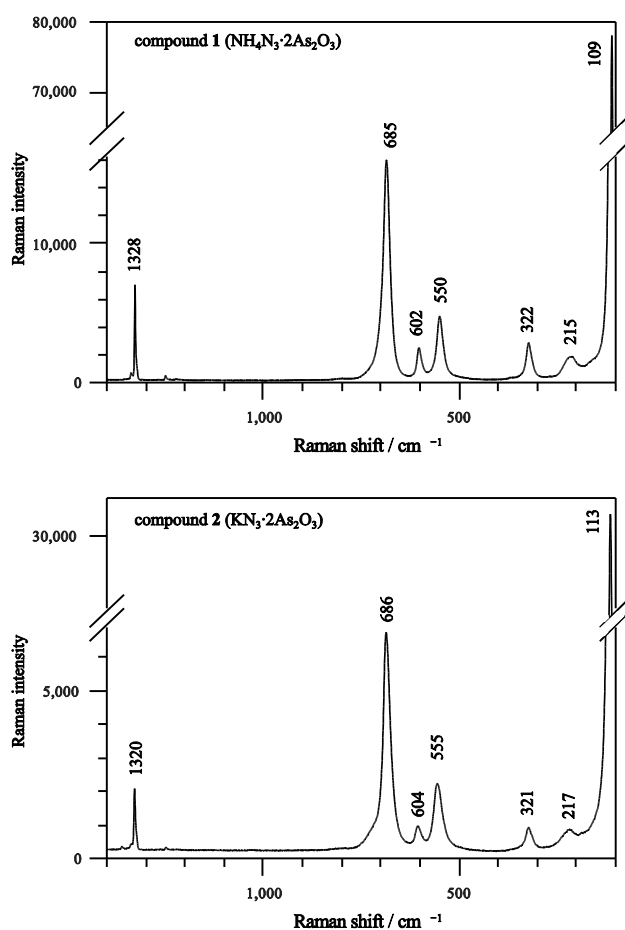


Fig. 3 Raman spectra of compounds **1** and **2**. Spectra in the whole registered wavenumber range are depicted in Fig. S3 in the Supporting Information.

and ammonium cations crystallise with As_2O_3 sheets displaying the same geometry.^{10,11} The only intercalate structure with different As_2O_3 sheet geometry is the one with NaBr, confirming the decisive role of cations in the shaping of arsenic(III) oxide sheets.¹² However, our attempts to obtain an intercalate with NaN_3 in an analogous procedure to the one described above proved unsuccessful.

Raman spectra

We have recorded Raman spectra of both compounds (Fig. 3) and performed quantum mechanical calculations to assign the observed bands to normal modes for compound **2** (see Table 2).^{23,41} The spectrum was evaluated computationally at Γ point using harmonic approximation. The polarised band located at 1329 cm^{-1} on the experimental spectrum corresponds to symmetric stretching of azide anions, whereas the remaining bands are due to As_2O_3 layers vibrations. The bands located at 686 , 604 , 554 , 321 and 217 cm^{-1} result from deformation vibrations of AsO_3 ψ -tetrahedra and the peak at 113 cm^{-1} corresponds to the vibrations of the whole As_2O_3 layers with respect to a rigid network of KN_3 . Fig. 4 shows eigenvectors associated with all normal modes of As_2O_3 layers vibrations and corresponding eigenvalues (harmonic frequencies). The agreement of the observed vibration frequencies with the theoretically predicted ones is excellent with the highest

Table 2 Assignment of compound **1** and **2** Raman bands (cm^{-1})

	symmetry	1 ^a		2		assignment
		$\text{NH}_4\text{N}_3 \cdot 2\text{As}_2\text{O}_3$ exp		$\text{KN}_3 \cdot 2\text{As}_2\text{O}_3$ B3LYP-D*	exp	
1	A_{1g}	109	p	97	113	δ_{sAsO_3}
2	E_{2g}	215	p	185	217	δ_{sAsO_3}
3	E_{1g}	322	p	318	321	δ_{sAsO_3}
4	E_{2g}	550	p	555	555	δ_{sAsO_3}
5	E_{1g}	602	p	607	604	δ_{sAsO_3}
6	A_{1g}	685	p	682	686	δ_{sAsO_3}
7	A_{1g}	1328	p	1323	1329	ν_{sN_3}
8		3190	p			N–H stretching

^a p stands for polarised

difference of 32 cm^{-1} (for the 185 cm^{-1} band) and the r.m.s. deviation of 14 cm^{-1} .

The Raman spectrum of compound **1** contains a peak at 3190 cm^{-1} which we attribute to N–H vibrations. The bands corresponding to As_2O_3 layers vibrations as well as to the symmetric stretching of azide anions are present in the spectrum of compound **1** and they are located at the same frequencies as in compound **2** within a few inverse centimetres range (see Table 2). This remarkable agreement is understandable given that the exchange of potassium for ammonium cation exercises a rather weak influence on As_2O_3 sheets. Consequently, we expect the frequencies of the As_2O_3 layers deformations to remain largely unchanged as different kinds of anions and cations are introduced into the crystal structure as long as the symmetry and topology of layers are retained.

The assignment for compound **1** was not attempted by comparison with the computationally predicted spectrum as

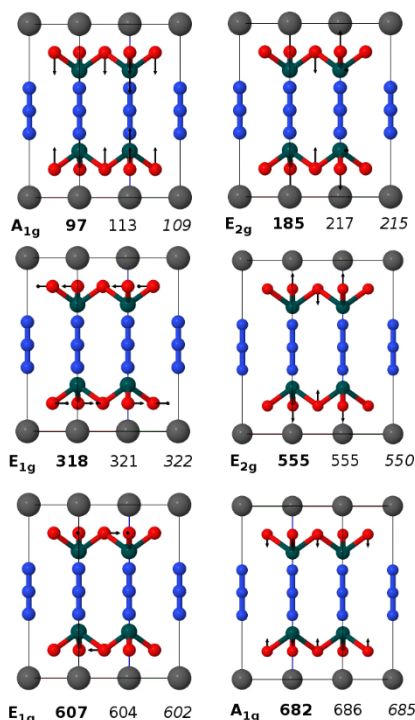


Fig. 4 Atomic displacements for normal modes of As_2O_3 sheets as calculated for intercalate **2**. The calculated harmonic frequencies as well as symmetry are given in bold, experimental frequencies for compounds **1** and **2** are given in normal font and italics, respectively.

calculations were carried out in the $P31m$ space group. Lowering of the symmetry, especially removal of inversion centre, has a significant impact on the spectrum and on the symmetry of vibrations, making comparison with experimental spectra very difficult. See Figure S3 and Tables S5 and S6 in the Supporting Information for more results concerning the frequencies calculations of intercalates **1** and **2**.

Conclusions

The synthesis and structural characterisation of the first As_2O_3 intercalates with a non-spherical anion is presented. The obtained compounds containing linear pseudohalogen azide anion are isotopic with the intercalates containing spherical halides. Spatial separation of ions by neutral As_2O_3 layers has been achieved and $\text{As} \cdots \text{N}_3^-$ contacts have been observed. Periodic DFT computations of interlayer interaction energies as well as the structural similarity of the coordination of K^+ and NH_4^+ cations by As_2O_3 sheets with their coordination by crown ethers indicates the templating effect of cations on arsenic(III) oxyanions and sheds light on the crystallisation process. It is the cations' interaction with As_6O_{12} cyclic units that is the decisive factor for the planar hexagonal As_2O_3 sheets formation. It has been confirmed by the computations that ionic bond is mainly responsible for holding layers together in crystals. Studied compounds are, therefore, an example of hybrid materials whose structure is governed by covalent bonds in two directions and by ionic bond in the third one. Last but not least, Raman spectrum of the intercalate **1** has been successfully predicted *ab initio* and all of the bands in both studied compounds have been assigned. The agreement between calculated and observed frequencies is very good.

Acknowledgements

This work was supported by the "Iuventus Plus" program of the Polish Ministry of Science and Higher Education (0242/IP3/2013/72). Calculations have been carried out using resources provided by Wroclaw Centre for Networking and Supercomputing (<http://wcss.pl>), grant No. 260. ChemMatCARS Sector 15 is principally supported by the National Science Foundation/Department of Energy under grant number NSF/CHE-0822838. Use of the Advanced Photon Source, an Office of Science User Facility operated for the U.S. Department of Energy (DOE) Office of Science by Argonne National Laboratory, was supported by the U.S. DOE under Contract No. DE-AC02-06CH11357. Raman spectra acquisition by Z. Żukowska, provision of the modified version of the EUGEN code by S. Tan and E. I. Pas (Izgorodina) and critical comments from M. Lesiuk are gratefully acknowledged.

Notes and references

^a Warsaw University of Technology, Faculty of Chemistry, Noakowskiego 3, 00-664 Warszawa, Poland, e-mail: piogun@ch.pw.edu.pl

^b University of Chicago, ChemMatCARS beamline, Advanced Photon Source, Argonne, Illinois 60439, United States.

† Electronic Supplementary Information (ESI) available: derived formulae for interlayer interaction energies, powder diffraction patterns and Raman spectra of compounds **1** and **2**, detailed results of geometry optimisations and frequencies calculations. See DOI: 10.1039/b000000x/

- ‡ **Crystal data for compound 1:** $2\text{As}_2\text{O}_3\cdot\text{NH}_4\text{N}_3$, $M = 455.76$ g/mol, $a = 5.2354(3)$ Å, $b = 5.2354(3)$ Å, $c = 9.6787(5)$ Å, $\alpha = 90^\circ$, $\beta = 90^\circ$, $\gamma = 120^\circ$, $V = 229.75(3)$ Å³, $T = 293(2)$ K, space group $P6/mmm$, $Z = 1$, $\mu(\text{MoK}\alpha) = 14.432$ mm⁻¹, 7048 reflections measured, 171 independent reflections ($R_{\text{int}} = 0.0493$). The final R_I and $wR(F^2)$ values ($I > 2\sigma(I)$) were 0.0155 and 0.0379, respectively. The final R_I and $wR(F^2)$ values (all data) were 0.0192 and 0.0388, respectively. The goodness of fit on F^2 was 1.220. **Crystal data for compound 2:** $2\text{As}_2\text{O}_3\cdot\text{KN}_3$, $M = 476.81$ g/mol, $a = 5.2425(10)$ Å, $b = 5.2425(10)$ Å, $c = 9.4865(17)$ Å, $\alpha = 90^\circ$, $\beta = 90^\circ$, $\gamma = 120^\circ$, $V = 225.79(10)$ Å³, $T = 45(2)$ K, space group $P6/mmm$, $Z = 1$, $\mu(\text{synchrotron}) = 2.872$ mm⁻¹, 775 reflections measured, 154 independent reflections ($R_{\text{int}} = 0.0236$). The final R_I and $wR(F^2)$ values ($I > 2\sigma(I)$) were 0.0220 and 0.0538, respectively. The final R_I and $wR(F^2)$ values (all data) were 0.0225 and 0.0539, respectively. The goodness of fit on F^2 was 1.356.
1. A. D. McNaught, A. Wilkinson, and International Union of Pure and Applied Chemistry, *Compendium of chemical terminology: IUPAC recommendations*, Blackwell Science, Oxford [England]; Malden, MA, USA, 1997.
 2. A. K. Padhi, K. S. Nanjundaswamy, and J. B. Goodenough, *J. Electrochem. Soc.*, 1997, **144**, 1188–1194.
 3. M. Winter, J. O. Besenhard, M. E. Spahr, and P. Novák, *Adv. Mater.*, 1998, **10**, 725–763.
 4. M. Rotter, M. Tegel, and D. Johrendt, *Phys. Rev. Lett.*, 2008, **101**, 107006.
 5. Z. A. Ren, J. Yang, W. Lu, W. Yi, G. C. Che, X. L. Dong, L. L. Sun, and Z. X. Zhao, *Mater. Res. Innov.*, 2008, **12**, 105–106.
 6. T. P. Ying, X. L. Chen, G. Wang, S. F. Jin, T. T. Zhou, X. F. Lai, H. Zhang, and W. Y. Wang, *Sci. Rep.*, 2012, **2**.
 7. A. Krzton-Maziopa, E. V. Pomjakushina, V. Y. Pomjakushin, F. von Rohr, A. Schilling, and K. Conder, *J. Phys. Condens. Matter*, 2012, **24**, 382202.
 8. A. Krzton-Maziopa and Z. Shermadini and E. Pomjakushina and V. Pomjakushin and M. Bendele and A. Amato and R. Khasanov and H. Luetkens and K. Conder, *J. Phys. Condens. Matter*, 2011, **23**, 052203.
 9. I. B. Rashkov, I. M. Panayotov, and V. C. Shishkova, *Carbon*, 1979, **17**, 103–108.
 10. F. Pertlik, *Monatshefte Für Chem.*, 1988, **119**, 451–456.
 11. M. Edstrand and G. Blomqvist, *Ark. För Kemi*, 1955, **8**, 245–256.
 12. F. Pertlik, *J. Solid State Chem.*, 1987, **70**, 225–228.
 13. P. A. Guñka, M. Dranka, and J. Zachara, *CrystEngComm*, 2011, **13**, 6163–6170.
 14. R. C. Clark and J. S. Reid, *Acta Crystallogr. Sect. A*, 1995, **51**, 887–897.
 15. *CrysAlisPro Software system*, Agilent Technologies UK Ltd, Oxford, UK, 2011.
 16. *APEX-II*, Bruker AXS Inc., Madison, Wisconsin, USA, 2012.
 17. G. M. Sheldrick, *Acta Crystallogr. Sect. A*, 2008, **64**, 112–122.
 18. O. V. Dolomanov, L. J. Bourhis, R. J. Gildea, J. A. K. Howard, and H. Puschmann, *J. Appl. Crystallogr.*, 2009, **42**, 339–341.
 19. *Diamond ver. 3.2i*, Crystal Impact GbR, Bonn, Germany, 1997.
 20. *Persistence of Vision (TM) Raytracer (POV-RAY)*, Persistence of Vision Pty. Ltd, Williamstown, Victoria, Australia, 2010.
 21. R. Dovesi, V. R. Saunders, C. Roetti, R. Orlando, C. M. Zicovich-Wilson, B. Pascale, B. Civalleri, K. Doll, N. M. Harrison, I. J. Bush, P. D'Arco, and M. Llunell, *CRYSTAL09*, University of Torino, Torino, 2009.
 22. R. Dovesi, R. Orlando, B. Civalleri, C. Roetti, V. R. Saunders, and C. M. Zicovich-Wilson, *Z. Für Krist.*, 2009, **220**, 571.
 23. F. Pascale, C. M. Zicovich-Wilson, F. López Gejo, B. Civalleri, R. Orlando, and R. Dovesi, *J. Comput. Chem.*, 2004, **25**, 888–897.
 24. P. Hohenberg and W. Kohn, *Phys. Rev.*, 1964, **136**, B864–B871.
 25. W. Kohn and L. J. Sham, *Phys. Rev.*, 1965, **140**, A1133–A1138.
 26. A. D. Becke, *J. Chem. Phys.*, 1993, **98**, 5648–5652.
 27. M. F. Peintinger, D. V. Oliveira, and T. Bredow, *J. Comput. Chem.*, 2013, **34**, 451–459.
 28. S. Grimme, *J. Comput. Chem.*, 2006, **27**, 1787–1799.
 29. B. Civalleri, C. M. Zicovich-Wilson, L. Valenzano, and P. Ugliengo, *CrystEngComm*, 2008, **10**, 405–410.
 30. C. G. Broyden, *Math. Comput.*, 1965, **19**, 577–593.
 31. D. D. Johnson, *Phys. Rev. B*, 1988, **38**, 12807–12813.
 32. P. Canepa, R. M. Hanson, P. Ugliengo, and M. Alfredsson, *J. Appl. Crystallogr.*, 2011, **44**, 225–229.
 33. A. Schulz and A. Villinger, *Inorg. Chem.*, 2009, **48**, 7359–7367.
 34. A. Schulz and A. Villinger, *Chem. – Eur. J.*, 2012, **18**, 2902–2911.
 35. R. Haiges, M. Rahm, D. A. Dixon, E. B. Garner, and K. O. Christe, *Inorg. Chem.*, 2012, **51**, 1127–1141.
 36. R. Haiges, M. Rahm, and K. O. Christe, *Inorg. Chem.*, 2013, **52**, 402–414.
 37. A. Simon and O. Reckeweg, *Z. Für Naturforsch. B*, 2003, **58b**, 1097–1104.
 38. E. D. Stevens, *Acta Crystallogr. Sect. A*, 1977, **33**, 580–584.
 39. E. Garman, *Acta Crystallogr. Sect. D*, 2010, **66**, 339–351.
 40. F. Corà, M. Alfredsson, G. Mallia, D. Middlemiss, W. Mackrodt, R. Dovesi, and R. Orlando, in *Principles and Applications of Density Functional Theory in Inorganic Chemistry II*, Springer Berlin Heidelberg, 2004, vol. 113, pp. 171–232.
 41. C. M. Zicovich-Wilson, F. Pascale, C. Roetti, V. R. Saunders, R. Orlando, and R. Dovesi, *J. Comput. Chem.*, 2004, **25**, 1873–1881.
 42. S. F. Boys and F. Bernardi, *Mol. Phys.*, 1970, **19**, 553–566.
 43. J. G. Brandenburg, M. Alessio, B. Civalleri, M. F. Peintinger, T. Bredow, and S. Grimme, *J. Phys. Chem. A*, 2013, **117**, 9282–9292.
 44. E. Madelung, *Phys. Z.*, 1918, **19**, 524.
 45. R. Hoppe, *Angew. Chem. Int. Ed. Engl.*, 1966, **5**, 95–106.
 46. R. Hoppe, *Adv. Fluor. Chem.*, 1970, **6**, 387.
 47. R. Hoppe, *Z. Naturforsch.*, 1995, **50a**, 555.
 48. L. Glasser, *Inorg. Chem.*, 2012, **51**, 2420–2424.
 49. E. I. Izgorodina, U. L. Bernard, P. M. Dean, J. M. Pringle, and D. R. MacFarlane, *Cryst. Growth Des.*, 2009, **9**, 4834–4839.
 50. The CSD (version 5.34 with updates, May 2013) search was restricted to complexes containing K^+ cation with at least one 18-crown-6 ether coordinated to it. Only structures with R factor lower than 0.05 and containing neither errors nor disorder were considered. The resulting data set comprises 554 entries.